Reversed Cherenkov emission of terahertz waves from an ultrashort laser pulse in a sandwich structure with nonlinear core and left-handed cladding

M. I. Bakunov,[1,2,*] R. V. Mikhaylovskiy,[1] S. B. Bodrov,[2,1] and B. S. Luk'yanchuk[3]

[1]*University of Nizhny Novgorod, Nizhny Novgorod 603950, Russia*
[2]*Institute of Applied Physics, Russian Academy of Sciences, Nizhny Novgorod, 603950, Russia*
[3]*Data Storage Institute, Agency for Science, Technology and Research, 117608 Singapore*
**bakunov@rf.unn.ru*

Abstract. We propose a scheme for an experimental verification of the reversed Cherenkov effect in left-handed media. The scheme uses optical-to-terahertz conversion in a planar sandwichlike structure that consists of a nonlinear core cladded with a material that exhibits left-handedness at terahertz frequencies. The focused into a line femtosecond laser pulse propagates in the core and emits Cherenkov wedge of terahertz waves in the cladding. We developed a theory that describes terahertz generation in such a structure and calculated spatial distribution of the generated terahertz field, its energy spectrum, and optical-to-terahertz conversion efficiency. The proposed structure can be a useful tool for characterization of the electromagnetic properties of metamaterials in the terahertz frequency range.

OCIS codes: (190.7110) Ultrafast nonlinear optics; (260.3090) Infrared, far; (230.4320) Nonlinear optical devices

References and links

1. V. E. Pafomov, “On transition radiation and the Vavilov-Cherenkov radiation,” Zh. Eksp. Teor. Fiz. **36**, 1853–1858 (1959) (Sov. Phys. JETP **9**, 1321 (1959)).
2. V. G. Veselago, “The electrodynamics of substances with simultaneously negative values of ε and μ,” Usp. Fiziol. Nauk **92**, 517–526 (1967) (Sov. Phys. USPEKHI **10**, 509–514 (1968)).
3. J. Lu, T. Grzegorczyk, Y. Zhang, J. Pacheco, Jr., B.-I. Wu, J. A. Kong, and M. Chen, “Cerenkov radiation in materials with negative permittivity and permeability,” Opt. Express **11**(7), 723–734 (2003).
4. Yu. O. Averkov, and V. M. Yakovenko, “Cherenkov radiation by an electron bunch that moves in a vacuum above a left-handed material,” Phys. Rev. B **72**(20), 205110 (2005).
5. Z. Y. Duan, Y. B. Gong, Y. Y. Wei, W. X. Wang, B.-I. Wu, J. A. Kong, and M. Chen, “Theoretical investigation into Cherenkov radiation in an anisotropic double-negative medium,” in *Proceedings of 33rd International Conference on Infrared, Millimeter, and Terahertz Waves*, (Pasadena, Calif., 2008).
6. Z. Y. Duan, B.-I. Wu, J. Lu, J. A. Kong, and M. Chen, “Reversed Cherenkov radiation in a waveguide filled with anisotropic double-negative metamaterials,” J. Appl. Phys. **104**(6), 063303 (2008).
7. Z. Y. Duan, B.-I. Wu, J. Lu, J. A. Kong, and M. Chen, “Cherenkov radiation in anisotropic double-negative metamaterials,” Opt. Express **16**(22), 18479–18484 (2008).
8. S. Antipov, L. Spentzouris, W. Gai, M. Conde, F. Franchini, R. Konecny, W. Liu, J. G. Power, Z. Yusof, and C. Jing, “Observation of wakefield generation in left-handed band of metamaterial-loaded waveguide,” J. Appl. Phys. **104**(1), 014901 (2008).
9. S. Xi, H. Chen, T. Jiang, L. Ran, J. Huangfu, B.-I. Wu, J. A. Kong, and M. Chen, “Experimental verification of reversed Cherenkov radiation in left-handed metamaterial,” Phys. Rev. Lett. **103**(19), 194801 (2009).
10. Z. Y. Duan, B.-I. Wu, S. Xi, H. S. Chen, and M. Chen, “Research progress in reversed Cherenkov radiation in double-negative metamaterials,” Progress In Electromagnetic Research **PIER 90**, 75–87 (2009).
11. G. A. Askar’yan, “Cherenkov radiation from optical pulses,” Phys. Rev. Lett. **57**(19), 2470 (1986).
12. S. B. Bodrov, M. I. Bakunov, and M. Hangyo, “Efficient Cherenkov emission of broadband terahertz radiation from an ultrashort laser pulse in a sandwich structure with nonlinear core,” J. Appl. Phys. **104**(9), 093105 (2008).
13. S. B. Bodrov, A. N. Stepanov, M. I. Bakunov, B. V. Shishkin, I. E. Ilyakov, and R. A. Akhmedzhanov, “Highly efficient optical-to-terahertz conversion in a sandwich structure with LiNbO3 core,” Opt. Express **17**(3), 1871–1879 (2009).
14. L. Peng, L. Ran, H. Chen, H. Zhang, J. A. Kong, and T. M. Grzegorczyk, “Experimental observation of left-handed behavior in an array of standard dielectric resonators,” Phys. Rev. Lett. **98**(15), 157403 (2007).

#120926 - $15.00 USD Received 3 Dec 2009; revised 24 Dec 2009; accepted 4 Jan 2010; published 14 Jan 2010

15. R. A. Shelby, D. R. Smith, and S. Schultz, "Experimental verification of a negative index of refraction," Science **292**(5514), 77–79 (2001).
16. S. O'Brien, and J. B. Pendry, "Photonic band-gap effects and magnetic activity in dielectric composites," J. Phys. Condens. Matter **14**(15), 4035–4044 (2002).
17. C. M. Soukoulis, M. Kafesaki, and E. N. Economou, "Negative-index materials: new frontiers in optics," Adv. Mater. **18**(15), 1941–1952 (2006).
18. L. Pálfalvi, J. Hebling, J. Kuhl, Á. Péter, and K. Polgár, "Temperature dependence of the absorption and refraction of Mg-doped congruent and stoichiometric $LiNbO_3$ in the THz range," J. Appl. Phys. **97**(12), 123505 (2005).
19. J. Hebling, A. G. Stepanov, G. Almási, B. Bartal, and J. Kuhl, "Tunable THz pulse generation by optical rectification of ultrasort laser pulses with tilted pulse fronts," Appl. Phys. B **78**, 593–599 (2004).
20. B. Bartal, I. Z. Kozma, A. G. Stepanov, G. Almási, J. Kuhl, E. Riedle, and J. Hebling, "Toward generation of μJ range sub-ps THz pulses by optical rectification," Appl. Phys. B **86**(3), 419–423 (2007).
21. M. I. Bakunov, S. B. Bodrov, A. V. Maslov, and M. Hangyo, "Theory of terahertz generation in a slab of electro-optic material using an ultrashort laser pulse focused to a line," Phys. Rev. B **76**(8), 085346 (2007).</jrn>

1. Introduction

One of the most intriguing electromagnetic phenomena in left-handed (LH) media is the reversed Cherenkov effect. Predicted by Pafomov as early as 1959 [1] (see also the famous paper by Veselago [2]), this effect started being studied in detail only recently. In Ref [3], Cherenkov radiation from a point charge in an isotropic LH medium, whose permittivity and permeability were modeled by Lorentz formulas, was calculated. It was shown, in accord with the prediction of Pafomov and Veselago, that the radiation pattern presents lobes in the backward direction – at the angles larger than 90° with respect to the charge velocity. In Ref [4], Cherenkov radiation of bulk and surface electromagnetic waves by a nonrelativistic electron bunch that moves above the surface of a model LH material was investigated. The effect of the LH material anisotropy on the spectral density and total radiated energy of reversed Cherenkov radiation was studied for a point charge moving in an unbounded anisotropic LH medium [5] and in a waveguide (partially) filled with such a medium [6,7]. In Ref [8], an indirect experimental observation of the reversed Cherenkov radiation from a beam of charged particles in a LH-medium-loaded waveguide was reported. In Ref [9], a waveguide with an array of slots was used to imitate the moving dipole, and backward radiation was detected after covering the array with a LH prism. Direct experimental verification of the reversed Cherenkov effect still remains a challenging problem [10].

In this paper we propose a feasible scheme for direct observation of the reversed Cherenkov radiation in the terahertz frequency range. To produce the Cherenkov radiation we propose to use an ultrashort laser pulse propagating in an electro-optic medium, rather than an electron bunch. The nonlinear polarization, produced by the pulse via nonlinear optical rectification, moves with the optical group velocity and emits terahertz radiation very much like a relativistic dipole [11]. To achieve the regime of the reversed Cherenkov radiation, we propose to sandwich a thin (of ~10 − 100 μm thickness) layer of a strongly nonlinear material, such as $LiNbO_3$, between two prisms made of a metamaterial exhibiting left-handedness in the terahertz frequency range (one of the prisms can be replaced by a substrate). To input the laser pulse into the structure, we propose to focus it by a cylindrical lens onto the facet of the nonlinear core so that the light line would be parallel to the plane of the structure. The laser pulse propagates in the core as a mode of the dielectric slab waveguide and emits Cherenkov wedge of terahertz waves in the LH prisms. The prisms are properly cut to output the radiation to vacuum. A similar sandwich structure but with ordinary right-handed (Si) cladding was recently proposed for highly efficient terahertz generation [12]. In Ref [13], using a Si-$LiNbO_3$-glass structure, 40 μJ, 50 fs Ti:sapphire laser pulses were converted into terahertz pulses of ~3 THz bandwidth with a record efficiency of over 0.1%.

Optical generation of the reversed Cherenkov radiation in the sandwich structure offers a number of advantages as compared to the schemes with electron bunches. First, the radiation power of Cherenkov radiation increases with its frequency; therefore, the terahertz frequency range is more fitted for detection than the microwave range. Second, focusing the pump laser beam into a line allows one to scale up the generated terahertz energy (using laser pulses with higher energy and increasing the length of the line in order to keep the laser intensity below

#120926 - $15.00 USD Received 3 Dec 2009; revised 24 Dec 2009; accepted 4 Jan 2010; published 14 Jan 2010

the damage threshold of the nonlinear core). Third, the radiation emitted by a line-source setup forms two beams having nearly flat wave fronts, i.e., Cherenkov wedge, rather than Cherenkov cone. The beams are linearly polarized with the electric field along the line source in the optimal case, as it will be shown below. This configuration fits well the typical design of metamaterials, for example, the dielectric rod-based metamaterial [14], unlike the rotational symmetry of the Cherenkov radiation from an electron bunch. And, finally, the optical-to-terahertz conversion scheme does not require a vacuum.

Below we develop a theory that describes terahertz generation in the sandwich structure with nonlinear core and isotropic LH cladding. We analyze the generated terahertz field, terahertz spectrum, and conversion efficiency for a specific structure with $LiNbO_3$ core and model Lorentz-type cladding pumped by Ti:sapphire laser (800 nm wavelength).

2. Generation scheme and model

The geometry of the structure and generation scheme are shown in Fig. 1. A thin layer ($|x| < a/2$, a ~10 – 100 μm) of a nonlinear material is sandwiched between two prisms ($|x| > a/2$) made of an isotropic metamaterial that exhibits negative permittivity and permeability at terahertz frequencies. For example, an array of high dielectric constant rods arranged along the y-axis can be used as a material of the prisms [14]. For the terahertz waves polarized along the y-axis and propagating in the x,z-plane such a metamaterial behaves as an isotropic medium. The pump laser pulse focused in the x-direction by a cylindrical lens is incident on the facet of the nonlinear core. The beam width in this direction is chosen to be ≈(0.2 – 0.3)a to optimize the excitation of the fundamental mode of the dielectric slab waveguide [12]. The laser pulse propagates in the + z-direction as the fundamental mode of the waveguide with the group velocity V and emits reversed (at the frequencies where the prism's material is left-handed) and direct (at other frequencies) Cherenkov radiation into the prisms. To transmit efficiently the terahertz waves into vacuum, the prisms are cut at the angles α and β (Fig. 1), which are to be defined below.

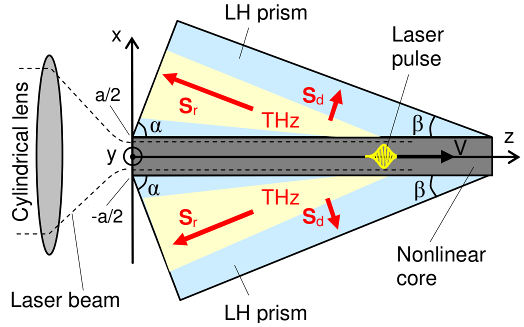

Fig. 1. Generation scheme. An optical pulse focused to a line propagates in the nonlinear core of the sandwich structure and excites Cherenkov wedge of terahertz waves in the output LH prisms. The arrows show the Poynting vector of the direct ($\mathbf{S})_d$) and reversed ($\mathbf{S})_r$) components of the Cherenkov radiation.

We use the same approximations as in Ref [12]. The structure, optical pulse, and terahertz fields are treated as two-dimensional [independent of y (Fig. 1)]. The optical pulse propagates in the core without distortions and has a Gaussian temporal envelope $F(\xi) = \exp(-\xi^2/\tau^2)$, where $\xi = t - z/V$ and τ is the pulse duration [the standard full-width at half maximum (FWHM) is $\tau_{\rm FWHM} = 2\sqrt{\ln 2}\tau \approx 1.7\tau$]. The dielectric slab waveguide is assumed to be oversized (a exceeds significantly the optical wavelength), therefore, the transverse intensity profile of the fundamental mode can be approximated as $G(x) = \cos^2(\pi x/a)$, $|x| < a/2$ and the velocity V is defined practically only by the material dispersion of the core: $V = c/n_g$, where n_g is the optical group refractive index of the core and c is the velocity of light. Transient effects at the entrance and exit boundaries of the sandwich are neglected.

#120926 - $15.00 USD Received 3 Dec 2009; revised 24 Dec 2009; accepted 4 Jan 2010; published 14 Jan 2010

The nonlinear polarization produced by optical rectification of the laser pulse in the core ($|x| < a/2$) can be written in the Fourier domain as

$$\tilde{\mathbf{P}}^{\mathrm{NL}} = \mathbf{p}(\omega)\tilde{F}(\omega)G(x), \quad \tilde{F} = \tau\big/(2\sqrt{\pi})\,\mathrm{e}^{-\omega^2\tau^2/4}, \tag{1}$$

where ω is the Fourier variable (frequency), which corresponds to ξ, and ˜ denotes quantities in the Fourier domain. We assume the optimal orientation of the amplitude vector $\mathbf{p}(\omega)$ – along the y axis, i.e., for $LiNbO_3$ core both the optical axis of $LiNbO_3$ and the laser pulse polarization are along the y axis. Such orientation of $\mathbf{p}(\omega)$ provides, first, most efficient terahertz generation [12] and, second, an appropriate polarization of the terahertz waves (with electric E_y and magnetic H_x, H_z field components) for the dielectric rod-based metamaterial [14]. The absolute value of $\mathbf{p}(\omega)$ is $p(\omega) = d_{eff}(\omega)E_0^2$, where $d_{eff}(\omega)$ is the effective nonlinear coefficient of the core's material ($d_{eff} = d_{33}$ for $LiNbO_3$) and E_0 is the maximum of the optical field envelope in the core.

To find the terahertz radiation generated by the nonlinear polarization (1), we use Maxwell's equations written in the frequency domain (all formulas in the paper are in cgs units),

$$\nabla_\omega \times \tilde{\mathbf{E}} = -\frac{i\omega}{c}\mu\tilde{\mathbf{H}}, \quad \nabla_\omega \times \tilde{\mathbf{H}} = \frac{i\omega}{c}\varepsilon\tilde{\mathbf{E}} + \frac{4\pi i\omega}{c}\tilde{\mathbf{P}}^{\mathrm{NL}}, \tag{2}$$

where the nabla operator ∇_ω has components $(\partial/\partial x, 0, -i\omega V^{-1})$ and the complex permittivity $\varepsilon(\omega, x)$ and complex permeability $\mu(\omega, x)$ in the terahertz range are $\varepsilon_c(\omega)$ and 1 in the core ($|x| < a/2$) and $\varepsilon_p(\omega)$ and $\mu_p(\omega)$ in the prisms ($|x| > a/2$), respectively.

For the permittivity and permeability of the metamaterial we use the generic forms [15]

$$\varepsilon_p(\omega) = 1 - \frac{\omega_{ep}^2 - \omega_{e0}^2}{\omega^2 - \omega_{e0}^2 - i\omega\gamma_e}, \quad \mu_p(\omega) = 1 - \frac{\omega_{mp}^2 - \omega_{m0}^2}{\omega^2 - \omega_{m0}^2 - i\omega\gamma_m}, \tag{3}$$

with the resonance frequencies ω_{e0} and ω_{m0}, plasma frequencies ω_{ep} and ω_{mp}, and damping rates γ_e and γ_m. Equations (3) are the standard Drude-Lorentz forms that are widely used for modeling of both metallic and dielectric metamaterials [3,4,15–17]. In particular, the effective permittivity and permeability of the dielectric-rod metamaterial exhibit the Lorentz-type resonance and isotropic behavior [14].

3. General solution

Projecting Eq. (2) into the coordinate system and eliminating $\tilde{H}_x$ and $\tilde{H}_z$ with use of

$$\tilde{H}_x = -\frac{n_g}{\mu}\tilde{E}_y, \quad \tilde{H}_z = -\frac{c}{i\omega\mu}\frac{\partial \tilde{E}_y}{\partial x}, \tag{4}$$

we obtain an equation for $\tilde{E}_y$,

$$\mu\frac{\partial}{\partial x}\left(\frac{1}{\mu}\frac{\partial \tilde{E}_y}{\partial x}\right) + \kappa^2\tilde{E}_y = -\frac{4\pi\mu\omega^2 p}{c^2}\tilde{F}(\omega)G(x). \tag{5}$$

In Eq. (5), we introduced the transverse wave vector $\kappa(\omega, x)$ given by

$$\kappa^2 = (\omega/c)^2[\varepsilon(\omega,x)\mu(\omega,x) - n_g^2]. \tag{6}$$

We solve Eq. (5) in the homogeneous regions $|x| < a/2$ and $|x| > a/2$ and match the solutions by the boundary conditions of continuity of $\tilde{E}_y$ and $\tilde{H}_z$ that arise after integrating Eq. (5) across the boundaries at $x = \pm a/2$.

We arrive at the following expressions for the electric field transform:

#120926 - $15.00 USD Received 3 Dec 2009; revised 24 Dec 2009; accepted 4 Jan 2010; published 14 Jan 2010

$$\tilde{E}_y = \begin{cases} C_1 e^{-i\kappa_p (x-a/2)}, & x > a/2 \\ C_2 e^{-i\kappa_c x} + C_3 e^{i\kappa_c x} + R(x), & |x| < a/2 \\ C_4 e^{i\kappa_p (x+a/2)}, & x < -a/2 \end{cases} \tag{7}$$

with

$$R(x) = \frac{2\pi\omega^2 p}{i\kappa_c c^2} \tilde{F} \int_{-a/2}^{a/2} dx' G(x') e^{-i\kappa_c |x-x'|}, \tag{8a}$$

$$C_2 = C_3 = C_1 e^{-ik_c a/2} [1 - \kappa_p (\kappa_c \mu_p)^{-1}]/2, \tag{8b}$$

$$C_1 = C_4 = \frac{2\pi\omega^2 p\tilde{F}(e^{i\kappa_c a/2} - e^{-i\kappa_c a/2})}{\kappa_c c^2 \Lambda[(\kappa_c a)^2 (2\pi)^{-2} - 1]}, \tag{8c}$$

$$\Lambda = (\kappa_p \mu_p^{-1} + \kappa_c) e^{i\kappa_c a/2} + (\kappa_p \mu_p^{-1} - \kappa_c) e^{-i\kappa_c a/2}. \tag{8d}$$

The coefficient κ_p is κ taken with $\varepsilon = \varepsilon_p$ and $\mu = \mu_p$ and κ_c is κ taken with $\varepsilon = \varepsilon_c$ and $\mu = 1$ [see Eq. (6)]. To ensure decay of the fields at $x \to \pm\infty$, Im κ_p should be taken negative for all frequencies. This also defines the sign of Re κ_p consistent with the condition of energy outflow from the core to $x \to \pm\infty$.

It follows from Eqs. (7) and (8c) that the emission of terahertz waves to the prisms is symmetric, $C_1 = C_4$.

To transform the solution (7)-(8) to the ξ domain we take inverse transform in the form

$$E_y(\xi, x) = \int_{-\infty}^{\infty} d\omega\, \tilde{E}_y(\omega, x) e^{i\omega\xi} \tag{9}$$

and the same formulas used for the other fields.

To find the terahertz energy emitted to the prisms from the unit area of the core-prism interfaces, i.e., the terahertz fluence, we integrate the $\pm x$-components of the Poynting vector $S_{\pm x} = \pm(c/4\pi) E_y H_z$ at $x = \pm a/2$ over infinite interval $-\infty < \xi < \infty$. This yields the fluence in one of the $\pm x$-directions,

$$W = \int_0^{\infty} d\omega\, w(\omega), \tag{10}$$

where $w(\omega)$ is the spectral density of fluence,

$$w(\omega) = (c^2/\omega) |C_1|^2 \,\mathrm{Re}(\kappa_p/\mu_p). \tag{11}$$

The total terahertz fluence is $2W$.

We introduce the optical-to-terahertz conversion efficiency per unit length of the sandwich structure (along the z-axis) as

$$\eta = W/W_{\mathrm{opt}}, \tag{12}$$

where $W_{\mathrm{opt}} = \pi^{1/2} I_0 a\tau/2$ is the energy of the pump optical pulse per unit length along the y-axis [$I_0 = (cn_c/8\pi)E_0^2$ is the peak optical intensity and n_c is the optical refractive index of the core].

#120926 - $15.00 USD Received 3 Dec 2009; revised 24 Dec 2009; accepted 4 Jan 2010; published 14 Jan 2010

4. Results and discussion

Let us now apply the general theory developed in Sec. 3 to a sandwich structure with $LiNbO_3$ core and metamaterial cladding [see Eq. (3)] pumped with Ti:sapphire laser (800 nm wavelength).

For $LiNbO_3$, we use the parameters of 0.68 mol% Mg-doped stoichiometric $LiNbO_3$ at room temperature, as in Ref [12]. The refractive index $n_{\mathrm{LN}} = \mathrm{Re}\,\varepsilon_c^{1/2}$ and amplitude absorption coefficient $\beta_{\mathrm{LN}} = (\omega/c)\,\mathrm{Im}\,\varepsilon_c^{1/2}$ of $LiNbO_3$ in the terahertz range are approximated by the following formulas (ν is in THz): $n_{\mathrm{LN}} = 4.94 + 0.021\nu^2 + 0.0012\nu^4$ [18] and $\beta_{\mathrm{LN}}[\mathrm{cm}^{-1}] = 24.83 - 12.68\nu + 15.91\nu^2$ (fitting of the data of Ref [18].). The optical refractive index and group refractive index of $LiNbO_3$ at 800 nm wavelength are $n_c = 2.16$ and $n_g = 2.23$, respectively [19]. The nonlinear coefficient of $LiNbO_3$ is $d_{33}[\mathrm{pm/V}] = 25 + 158 \times |1 - \omega^2/\omega_{\mathrm{TO}}^2 - i\gamma\omega/\omega_{\mathrm{TO}}^2|^{-1}$ with $\omega_{\mathrm{TO}}/(2\pi) = 7.68$ THz and $\gamma/(2\pi) = 0.1$ THz [20].

For the metamaterial, we set $\omega_{e0} = \omega_{m0} = 2\pi \times 1$ THz, $\omega_{ep} = \omega_{mp} = 2\pi \times 4$ THz, and $\gamma_e = \gamma_m = 2\pi \times 0.01$ THz in Eq. (3). Using the model with $\varepsilon_p(\omega) = \mu_p(\omega)$, like in Ref [3], simplifies the analysis without changing the characteristic features of the radiation. A brief discussion of the case $\varepsilon_p(\omega) \neq \mu_p(\omega)$ will be given in the end of the section. Figure 2 shows the real and imaginary parts of the refractive index $n_p = (\varepsilon_p \mu_p)^{1/2} = \varepsilon_p$ as functions of ω. The condition of left-handedness Re $n_p < 0$ is fulfilled in the frequency interval $1 < \omega/(2\pi) < 4$ THz. The conditions Re $n_p > n_g$ and Re $n_p < -n_g$ define the frequency intervals $0 < \omega/(2\pi) < 1$ THz and $1 < \omega/(2\pi) < 2.37$ THz where the direct and reversed Cherenkov radiations, respectively, occur. In the vicinity of the resonance, at $\omega/(2\pi) \approx 1$ THz, the radiation is suppressed by a large (negative) value of Im n_p.

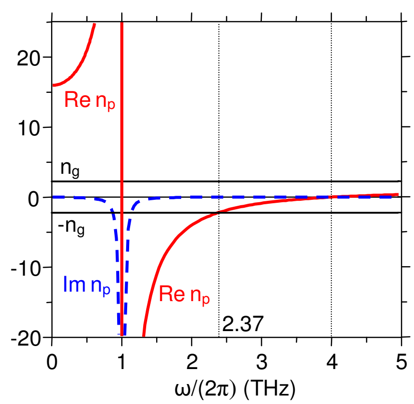

Fig. 2. Real (solid) and imaginary (dashed) parts of $n_p = \varepsilon_p = \mu_p$ as functions of ω.

Figure 3(a) shows the spatial distribution of the electric field E_y calculated numerically on the basis of Eqs. (7), (8), and (9) for a sandwich structure with $a = 40$ μm. The radiation pattern in Fig. 3(a) is a superposition of the wavefronts corresponding to the direct [with frequencies of $0 < \omega/(2\pi) < 1$ THz] and reversed [with frequencies of $1 < \omega/(2\pi) < 2.37$ THz] components of Cherenkov radiation. To get an insight into the radiation pattern, it is instructive to plot separately the wavefronts of the direct [Fig. 3(b)] and reversed [Fig. 3(c)] components of the Cherenkov radiation.

#120926 - $15.00 USD Received 3 Dec 2009; revised 24 Dec 2009; accepted 4 Jan 2010; published 14 Jan 2010

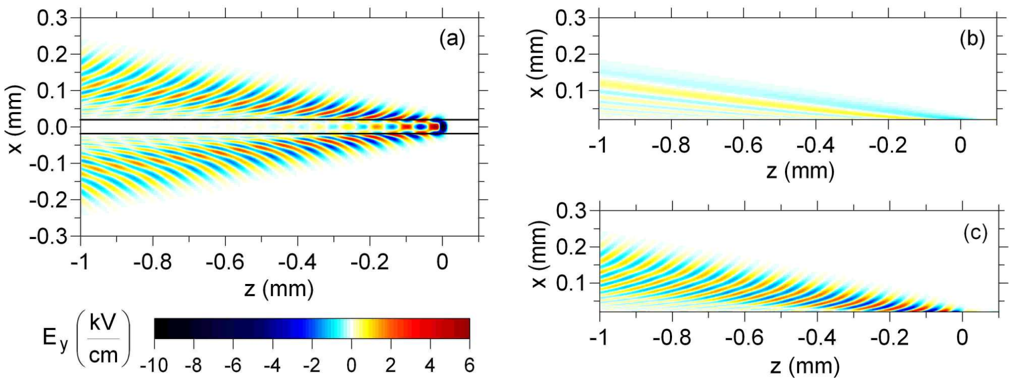

Fig. 3. (a) Snapshot of the electric field $E_y(x,z,t)$ at $t = 0$ produced in a sandwich structure with $a = 40$ μm by a Ti:sapphire laser pulse with duration $\tau_{FWHM} = 100$ fs and peak intensity $I_0 = 40$ GW/cm^2 ($W_{opt} = 8.5$ μJ/cm). The core boundaries are shown with the horizontal lines. (b,c) The components of the radiation pattern in the output prism corresponding to direct (b) and reversed (c) Cherenkov radiation.

The radiation pattern of the direct component [Fig. 3(b)] resembles that for a Si-LiNbO$_3$-Si structure [12]. The pattern in Fig. 3(b) is, however, affected by the dispersion of the metamaterial prisms, contrary to practically dispersionless Si in Ref [12]. Indeed, in Fig. 3(b) the wavefronts of partial plane waves with higher frequencies are oriented at smaller angles θ with respect to the z-axis, in accord with the formula $\tan\theta = \omega n_g / [c \operatorname{Re}\kappa_p(\omega)]$ [see also Fig. 4(a)]. The opening angle of the direct Cherenkov cone $\theta_d \approx 8°$ corresponds to zero frequency, $\sin\theta_d = n_g / \varepsilon_p(0)$ with $\varepsilon_p(0) = (\omega_{ep}/\omega_{e0})^2 = 16$.

The radiation pattern of the reversed component of the Cherenkov radiation [Fig. 3(c)] differs significantly from the ones in Ref [12]. and in Fig. 3(b). The wavefronts of the reversed component are almost perpendicular to the Cherenkov cone [cf. Figure 3(b)]. This corresponds to negative values of $\operatorname{Re}\kappa_p(\omega)$ in the formula for partial plane waves $\tan\theta = \omega n_g / [c \operatorname{Re}\kappa_p(\omega)]$ [see also Fig. 4(a)]. The radiation pattern as a whole moves with time along the z-axis with the optical pulse velocity. The component of this velocity along the normal to a wavefront, which determines the phase velocity of a partial plane wave, is directed towards the z-axis, in accord with the predictions of Pafomov [1] and Veselago [2]. For the parameters used, the reversed component of the Cherenkov radiation has stronger fields than the direct component [cf. Figures 3(b) and (c)] and, as a result, it dominates in the total radiation pattern [Fig. 3(a)].

In the far field zone (at large ξ) integral (9) can be asymptotically evaluated using the stationary phase method [21]. The most informative for interpreting the radiation patterns in Fig. 3 is the dependence of the stationary frequency ω_s on the angle θ, a half-apex angle of a cone with its apex on the moving laser pulse $\xi = 0$ [21],

$$V \frac{d}{d\omega} \operatorname{Re}\kappa_p = \frac{V\xi}{|x|} = \cot\theta. \qquad (13)$$

The dependence $\omega_s(\theta)$ is shown in Fig. 4(b). For the direct component of the Cherenkov radiation [$0 < \omega/(2\pi) < 1$ THz], the dependence $\omega_s(\theta)$ is similar to $\omega(\theta)$ in Fig. 4(a), i.e., ω_s decreases with θ tending to zero at the maximal angle (the opening angle of the direct Cherenkov cone) $\theta_d \approx 8°$. For the reversed component of the Cherenkov radiation [$\omega/(2\pi) > 1$ THz], the maximal angle θ_r, i.e., the opening angle of the reversed Cherenkov cone, is $\theta_r \approx 10°$, which agrees well with Fig. 3(c). For $\theta < \theta_r$, the function $\omega_s(\theta)$ is double-valued. The higher-frequency branch defines the fine structure of the wavefronts in Fig. 3(c), whereas the lower-frequency branch gives rise to the large-scale modulation of the radiation pattern visible in Fig. 3(c).

#120926 - $15.00 USD Received 3 Dec 2009; revised 24 Dec 2009; accepted 4 Jan 2010; published 14 Jan 2010

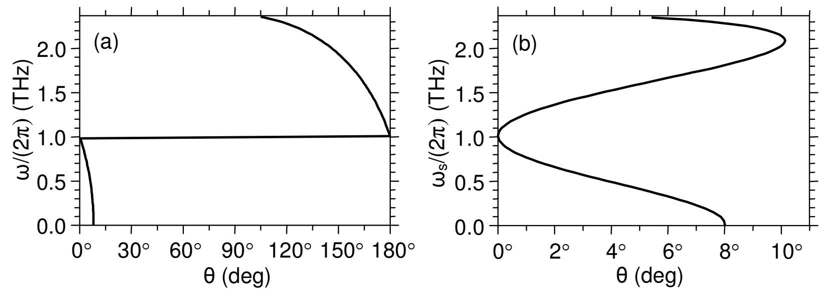

Fig. 4. The frequency ω of a partial plane wave (a) and the stationary frequency ω_s (b) as functions of θ.

Completing the discussion of the radiation pattern, to output efficiently the direct and reversed components of the Cherenkov radiation to vacuum the metamaterial prism should be cut with its edges parallel to the wavefronts of the components, i.e., at $\alpha \approx 20° - 60°$ (depending on the frequency to be outputted most efficiently) for the reversed component and $\beta \approx 8°$ for the direct component (Fig. 1). To specify the optimal angle α more accurately, one needs to calculate the spectrum of the reversed Cherenkov component and tune α to its maximal frequency.

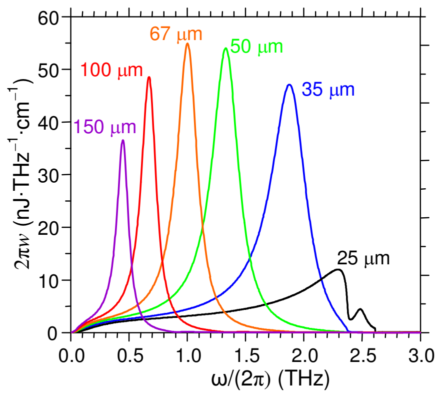

Fig. 5. The spectral density of terahertz fluence $2\pi w[\omega/(2\pi)]$ for different a (shown near the corresponding curves). The peak optical intensity is fixed to I_0 = 40 GW/cm^2 for all curves and τ_{FWHM} = 100 fs.

Figure 5 shows the spectral density of terahertz fluence $w(\omega)$ calculated using Eq. (11) for different core thicknesses a and fixed peak optical intensity I_0 (for convenience of practical use, we plot $2\pi w[\omega/(2\pi)]$ rather than $w(\omega)$ in Fig. 5). For $a \approx 30 - 67$ μm, $w(\omega)$ has a pronounced peak in the frequency band of the reversed Cherenkov radiation $1 < \omega/(2\pi) < 2.37$ THz; the thicker the core, the lower the peak's frequency. For a = 67 μm, the peak falls at 1 THz. Due to strong resonant absorption in the prisms at 1 THz (Fig. 2) the peak will split rapidly into two with distance from the core (similar splitting at 1 THz will be experienced by the wings of the other curves in Fig. 5). For $a > 67$ μm, the peak shifts to the frequency band of the direct Cherenkov radiation $0 < \omega/(2\pi) < 1$ THz and, for $a > 150$ μm, it quits the terahertz frequency range. For $a < 30$ μm, the spectrum exhibits no peaks. For $30 < a < 150$ μm, the height of the peak varies with a only slightly. Mathematically, the peak in the spectrum appears due to the factor $|\Lambda(\omega)|^{-2}$ in Eq. (11). From the physical point of view, the existence of the peak can be attributed to constructive interference of the terahertz waves emitted from the core directly and after multiple reflections at the core-prism boundaries. For $a < 30$ μm, the peak falls into the frequency band $\omega/(2\pi) > 2.37$ THz, where Cherenkov radiation is prohibited (Fig. 2), and the contribution of $|\Lambda(\omega)|^{-2}$ into $w(\omega)$ is suppressed by the factor $\mathrm{Re}(\kappa_p/\mu_p)$, which is negligible in this frequency band. If we fix the optical pulse energy

#120926 - $15.00 USD Received 3 Dec 2009; revised 24 Dec 2009; accepted 4 Jan 2010; published 14 Jan 2010

W_{opt}, rather than the intensity I_0, the peak will decrease with increasing a due to decrease of I_0 and, therefore, of p in Eq. (11).

Let us now calculate the terahertz fluence and optical-to-terahertz conversion efficiency per unit length of the structure. Dividing the integration range in Eq. (10) into two intervals $0 < \omega/(2\pi) < 1$ THz and $1 < \omega/(2\pi) < 2.37$ THz [$w(\omega)$ is negligible at $\omega/(2\pi) > 2.37$ THz] we represent the total terahertz fluence W as a sum of the fluences provided by the direct (W_d) and reversed (W_r) components of the Cherenkov radiation: $W = W_d + W_r$. Correspondingly, the efficiency η can be written as a sum of efficiencies $\eta = \eta_d + \eta_r$ with $\eta_d = W_d/W_{\mathrm{opt}}$ and $\eta_r = W_r/W_{\mathrm{opt}}$ [see Eq. (12)].

Figure 6 shows the terahertz fluences W_r [Fig. 6(a)] and W_d [Fig. 6(b)], evaluated using Eqs. (10) and (11), as functions of a and τ_{FWHM} for the fixed peak optical intensity $I_0 = 40$ GW/cm^2. According to Fig. 6(a), the fluence W_r has a broad maximum with $W_r \approx 50 - 60$ nJ/cm at $a \approx 40 - 60$ μm (this agrees with Fig. 5) and $\tau_{\mathrm{FWHM}} \approx 200 - 400$ fs. In this range of the parameters, $W_d < W_r$ [Fig. 6(b)]. For $a > 65$ μm, W_d dominates over W_r; maximal W_d is reached at a value of a that increases from 75 to 110 μm with increasing τ_{FWHM} from 100 to 500 fs, respectively.

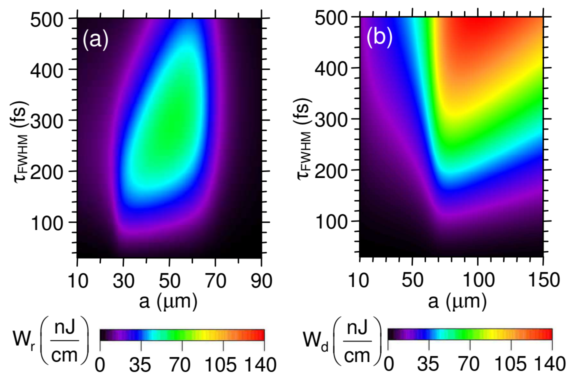

Fig. 6. The terahertz fluences (a) W_r and (b) W_d as functions of a and τ_{FWHM} for the fixed peak optical intensity $I_0 = 40$ GW/cm^2.

Figure 7 shows the conversion efficiencies η_r [Fig. 7(a)] and η_d [Fig. 7(b)], evaluated using Eqs. (10), (11), and (12), as functions of a and τ_{FWHM} for the fixed energy of the optical pulse $W_{\mathrm{opt}} = 8.5$ μJ/cm. Both efficiencies η_r and η_d decrease with increasing τ_{FWHM} due to a decrease in the peak optical intensity I_0 and, therefore, in p. For a given τ_{FWHM}, there is a narrow interval of a around $a \approx 30$ μm (for example, $28 < a < 32$ μm for $\tau_{\mathrm{FWHM}} = 100$ fs), where η_r reaches a maximum and significantly exceeds η_d. This interval shrinks to $a \approx 30$ μm with increasing τ_{FWHM} [Fig. 7(a)]. According to Fig. 7(a), even for a moderate peak optical intensity of $I_0 \approx 50$ GW/cm^2 ($W_{\mathrm{opt}} = 8.5$ μJ/cm, $\tau_{\mathrm{FWHM}} = 100$ fs, and $a = 30$ μm), the efficiency η_r can be as high as $\eta_r \approx 0.005$ cm^{-1}. A boost of η_r and η_d at $a \approx 10$ μm can be explained by a growth of I_0 with decreasing a. For $a \approx 10$ μm, the generated terahertz spectrum exhibits no peaks, it becomes flat in the frequency band of $0.5 < \omega/(2\pi) < 2$ THz. However, so thin cores are inconvenient for practical use because of difficulties with focusing the pump laser beam onto the core facet.

#120926 - $15.00 USD Received 3 Dec 2009; revised 24 Dec 2009; accepted 4 Jan 2010; published 14 Jan 2010

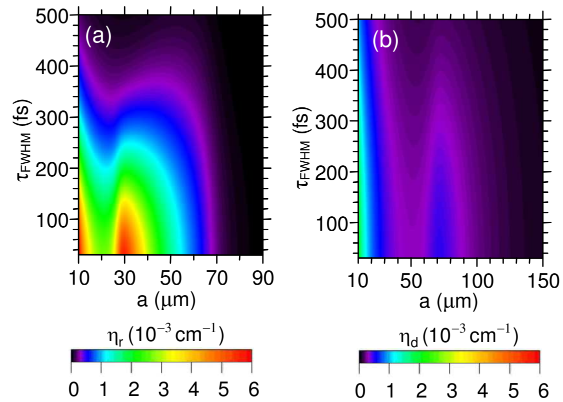

Fig. 7. The conversion efficiencies (a) η_r and (b) η_d as functions of a and τ_{FWHM} for the fixed optical pulse energy W_{opt} = 8.5 μJ/cm.

Let us discuss briefly the case $\varepsilon_p(\omega) \neq \mu_p(\omega)$. Assuming for definiteness that the characteristic frequencies in Eq. (3) are $\omega_{m0}/(2\pi)$ = 1 THz, $\omega_{e0}/(2\pi)$ = 2 THz, $\omega_{mp}/(2\pi)$ = 4 THz, and $\omega_{ep}/(2\pi)$ = 5 THz, we obtain that a stop band $1 < \omega/(2\pi) < 2$ THz, where Re $\varepsilon_p > 0$ and Re $\mu_p < 0$, appears between the frequency bands of the direct [$0 < \omega/(2\pi) < 1$ THz] and reversed [$2 < \omega/(2\pi) < 2.8$ THz] Cherenkov radiation. For $a < 40$ μm, the spectral density $w(\omega)$ is concentrated mainly in the frequency band of the reversed radiation, reaching maximum values at $a \approx 20 - 30$ μm (for a fixed peak optical intensity). In the frequency band of the direct radiation, $w(\omega)$ becomes noticeable for $a > 40$ μm. For another set of characteristic frequencies $\omega_{m0}/(2\pi)$ = 2 THz, $\omega_{e0}/(2\pi)$ = 1 THz, $\omega_{mp}/(2\pi)$ = 5 THz, and $\omega_{ep}/(2\pi)$ = 4 THz, the frequency bands of the direct/reversed radiation and the stop band remain the same as in the previous example but distribution of $w(\omega)$ between the frequency bands becomes somewhat different. Whereas the reversed radiation is maximized at the same value of $a \approx 30$ μm, $w(\omega)$ in the frequency band of the direct radiation is now considerable in the wide range of a, i.e., for $a > 10$ μm, and dominates over the reversed radiation for $a > 35$ μm. For both sets of the characteristic frequencies the radiation patterns remain qualitatively similar to Fig. 3(a).

5. Conclusion

To conclude, we have proposed a scheme for experimental verification of the reversed Cherenkov effect. This scheme uses emission of terahertz waves by optical rectification of the femtosecond laser pulse propagating in a sandwichlike structure with nonlinear core and LH cladding. The scheme offers a number of advantages as compared to the schemes with electron bunches: (i) exploiting the terahertz frequency range instead of microwaves increases the radiation power, (ii) focusing the pump laser beam into a line allows one to scale up the generated terahertz energy and (iii) forms more convenient for practical implementation Cherenkov wedge, rather than Cherenkov cone, (iv) the generated spectrum can be tuned by changing the thickness of the nonlinear core, and (v) the scheme does not require a vacuum. A proper cutting of the output metamaterial prism allows one to output the direct and reversed components of the Cherenkov radiation in separate (almost perpendicular) directions.

To demonstrate the efficiency of the scheme, we developed a theory that describes Cherenkov radiation in a sandwich structure with LH cladding. The theory allows one to calculate spatial distribution of the generated terahertz field, terahertz energy spectrum, and optical-to-terahertz conversion efficiency.

Applying the developed theory to a structure with $LiNbO_3$ core and cladding made of a metamaterial with Lorentzian dielectric permittivity and permeability we predicted the internal conversion efficiency into the reversed component of Cherenkov radiation of up to 0.5% in a 1 cm long and 1 cm wide structure with a 30 μm thick core pumped by Ti:sapphire laser

Received 3 Dec 2009; revised 24 Dec 2009; accepted 4 Jan 2010; published 14 Jan 2010

with ~100 fs pulse duration and 8.5 μJ pulse energy. The generated frequency spectrum has a peak of ~0.4 THz width at ~2 THz.

The proposed structure can be a useful tool for characterization of the electromagnetic properties of metamaterials in the terahertz frequency range.

Acknowledgments

This work was supported in part by RFBR Grant Nos. 08-02-92216 and 09-02-12324. Two of the authors (M.I.B. and B.S.L.) gratefully acknowledge support from the THz S&T Inter-RI Program, project 082 141 0039 funded by A*STAR-SERC, Singapore.

#120926 - $15.00 USD Received 3 Dec 2009; revised 24 Dec 2009; accepted 4 Jan 2010; published 14 Jan 2010